# ACOUSTIC EMISSION ANALYSIS TO RECOGNIZE THE FRACTURE PATTERN OF REFRACTORY MATERIALS DURING THERMAL SHOCK

Emilie Dahlem, Christian Dannert
Forschungsgemeinschaft Feuerfest e.V., Höhr-Grenzhausen, Germany

**ABSTRACT**
The disc irradiation method is a thermal shock testing method developed by Forschungsgemeinschaft Feuerfest e.V. at the European Centre for Refractories (ECREF), Höhr-Grenzhausen, Germany, to recognise the fracture pattern of refractory materials with high resistance to thermal shock. Using the disc irradiation method, the critical thermal shock stress of refractory materials under ascending thermal shock conditions can be reached. During the thermal shock itself, the characteristic acoustic emissions (AE) due to crack initiation and propagation in refractories are being recorded. A clustering method was established in order to identify, from the recorded AE, the crack formation and evolution processes in number of alumina based materials with different failure processes during thermal shock.

**KEYWORDS**
Thermal shock, acoustic emission, pattern recognition, refractories, disc irradiation method

**INTRODUCTION**
Refractories are materials essential for all highly industrialized processes which are performed at elevated temperatures. In use, the refractories are often heated up rapidly due to the demands of these industrial processes, and this can damage the refractory lining. As a result, its service life and thus the uninterrupted operation of the industrial processes are reduced. This is why it is worthwhile to develop new refractory lining materials with improved resistance to thermal shock at high temperatures.
To optimise the thermal shock resistance of refractories, it is necessary to identify and characterise as precisely as possible the damage evolution of these materials during thermal shock. Such information will then allow predicting the behaviour of refractory structures by the use of models. Non-destructive experimental characterisations nowadays promise major advantages for studying the damage processes of refractories.
Acoustic emissions (AE) testing is a recognized non-destructive test (NDT) method commonly used to detect and locate faults in mechanically loaded structures and components. The method has been developed and applied to numerous structural components, such as steam pipes and pressure vessels, and in the research areas of rocks, composite materials and metals [1, 2]. The energy released during a damage process is detected by piezoelectric sensors in form of transient elastic waves. About 15 waveform parameters (amplitude, energy, counts…) can be studied from the acquired waves. This information can be then used to correlate the acoustic emission activity with the damage evolution inside of the materials under test. Previous work has shown that damage in composite materials, such as matrix cracking, fibre cracking or interfacial debonding, can be identified by the use of acoustic emission [3, 4].
With suitable methods for in-situ damaging detection, for instance microphones, the thermal shock disc irradiation method at Forschungsgemeinschaft Feuerfest e.V. was being developed further to investigate fracture processes taking place within refractory test pieces during thermal shock.
Using in situ detection of the AE during cracking, the different fracture pattern in the stressed refractory test piece (cracks propagating through the matrix, the grains, the interface) can be identified by analysing the acoustic emissions due to the fracture mechanisms during the thermal shock procedure. The k-means method is applied to classify and identify the AE signals emitted by damage mechanisms. Such fracture analysis allows developing a new generation of refractory linings with a higher thermal shock resistance.

**MATERIAL AND EXPERIMENTAL PROCEDURE**
**Refractory material description and material preparation**
For this study, two series of material have been prepared at IKGB, Freiberg, Germany: four alumina compositions with different maximum grain sizes (0.01 to 0.5 mm) (see Table 1) and four alumina compositions with even higher maximum grain sizes (0.5 to 6 mm) (see Table 2). The purpose of changing the maximum particle size and the maximum grain size in the two series was to provoke different fracture patterns.
The raw materials used for this investigation were tabular and reactive alumina (99.5 % $Al_2O_3$; Almatis, Ludwigshafen, Germany).

Tab. 1: Compositions of the first series of samples investigated within this study.

| Raw Material | Particle size | A5 | A50 | A200 | A500 |
|---|---|---|---|---|---|
| | mm | wt.-% | | | |
| T60/64 | 0 – 0.5 | 0 | 0 | 0 | **36** |
| T60/64 | 0 – 0.2 | 0 | 0 | **90** | 52 |
| T60/64 | 0 – 0.045 | 0 | **75** | 0 | 0 |
| T60/64 | 0 – 0.020 | 0 | 25 | 9 | 0 |
| CT9FG | 0 – 0.028 | 0 | 0 | 0 | 12 |
| CTC3000SG | 0 – 0.004 | 0 | 0 | 1 | 0 |
| CL370 | 0 – 0.010 | **100** | 0 | 0 | 0 |

Tab. 2: Compositions of the second series of samples investigated within this study.

| Raw Material | Particle size | A05-F | A1-F | A3-F | A6-F |
|---|---|---|---|---|---|
| | mm | wt.-% | | | |
| T60/64 | 3 – 6 | 0 | 0 | 0 | **36** |
| T60/64 | 1 - 3 | 0 | 0 | **40** | 12 |
| T60/64 | 0.5 – 1 | 0 | **30** | 7 | 14 |
| T60/64 | 0.2 – 0.6 | **37** | 0 | 0 | 0 |
| T60/64 | 0 – 0.5 | 0 | 15 | 10 | 0 |
| T60/64 | 0 – 0.2 | 34 | 30 | 26 | 25 |
| T60/64 | 0 – 0.020 | 8 | 9 | 0 | 0 |
| CL370 | 0 – 0.010 | 18 | 13 | 14 | 10 |
| Alphabond | | 3 | 3 | 3 | 3 |
| Water* | | 7.5 | 6.4 | 5.3 | 4.8 |

** with respect to the solid content*

The first four compositions were mixed in an intensive mixer (Maschinenfabrik Gustav Eirich, Hardheim, Germany) and cold isostatically pressed at 100 MPa. The second series of samples were prepared as self-flowing castables. The grain size distribution of these compositions was chosen according to Fruhstorfer et al. with n = 0.28 and $n_{max}$ = 0,8. The authors showed for a 3 mm castable that the porosity and density reached optimal values for these parameters. That is why the water content was reduced significantly. The compositions were mixed in a labora-

tory mixer (Tonitechnik, Germany). Afterwards they were poured into cylindrical moulds. The test pieces were fired up to 1600 °C and cylinders of 75 mm in diameter and 100 mm in height were cut out of the sintered bulk bodies. Out of these cylinders, discs for the thermal shock investigation were cut.

**Experimental procedure: Disk irradiation method**

The disc irradiation method was first developed in the 1980s in order to determine the critical thermal shock stress intensity factor of technical ceramics under ascending thermal shock conditions [5]. Since then, the test principle and test piece geometry were further developed to investigate the specific behaviour of refractory products under thermal loading and the method was set up at Forschungsgemeinschaft Feuerfest e.V.

The disc-shaped test pieces (diameter of about 75 mm and thickness of at least 5 mm) are irradiated centrally on both sides using focused halogen lamps (Figure 1) [6]. During the thermal shock process, the temperatures in the centre and at the edge of each test pieces are measured online in a contactless way thanks to pyrometers. Intensity of the thermal shocks can be adjusted by varying the power going to the halogen lamps so the resulting temperature difference between the centre and the edge of the test piece is reduced or increased accordingly.

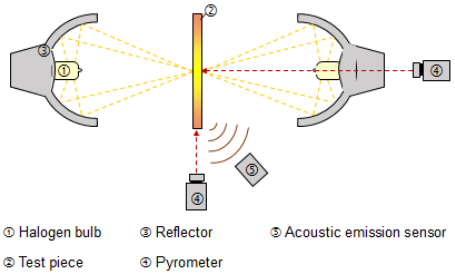


Fig. 1: Disc irradiation method.

Within a few seconds after switching on the halogen lamps, a circular temperature field is generated in the test piece (Figure 2). The temperature difference between centre and edge depends mainly on the thermal conductivity of the tested material and is usually greater than 500 K in the first stage of the thermal shock. The heating-up regime causes a higher thermal expansion at the heated centre of the test piece compared to its edge, inducing a stress gradient in the test piece.

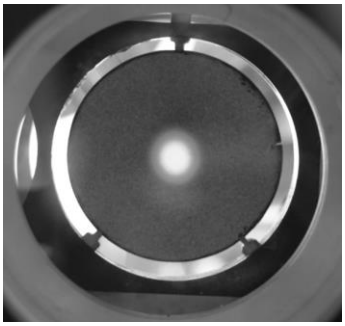

Fig. 2: Test piece immediately after irradiation heating.

Finite Element Simulations have been carried out on this testing method in order to determine the viability of the test with the proposed test piece design and to estimate the temperature distribution and the stress distribution within the test piece as a function of time. A simplified two-dimensional axisymmetric plane was considered for the model since the test piece geometry exhibit radial symmetry. The test piece was heated with the radiation mode by taking into account the corresponding surface emissivity of the ceramic and the carbon layer. The simulated temperatures showed good matching with the temperatures measured online during the tests. More information of the FEM results are available in [7].

The tensile stresses in the circular direction at the edge region of the test pieces increase progressively during the testing procedure. These stresses ultimately induce the fracture of the test pieces, which is typically initiated at the edge and propagates towards the centre.

**Calibration and data acquisition**

AE data was recorded during the thermal shock procedures using an AE sensor, placed about 10 cm from the sample without contact. Part of the ambient noise was filtered using a threshold of 30 dB. After the calibration step, AE signals were captured during thermal shocks of samples with different compositions (Table 1). Signal descriptors ("AE parameters") such as rise time, counts, energy, duration, amplitude and counts to peak (Figure 3) were evaluated from the AE signals. The energy, for example, is represented by the area below the detection signal envelope line in Figure 3.

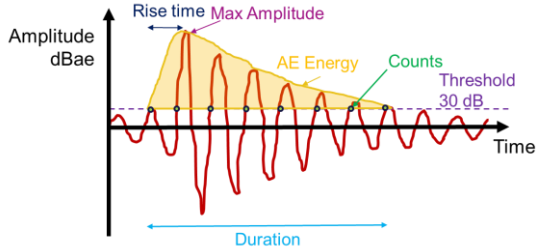


Fig. 3: Typical AE signal and AE parameters.

**Pattern recognition method of AE**

Pattern recognition techniques were applied by the use of k-means algorithm for acoustic emission signal classification. The aim was to identify sets of AE parameters that occur during different fracture patterns. For instance, previous work [1] has shown that fibre breakings, interphase failures and matrix cracking can be identified separately by this way.

K-means is a simple iterative algorithm, aiming at minimizing the square error for a given number of clusters. The algorithm, starting with the initial number of clusters specified, assigns the remaining points to one of the predefined clusters by nearest neighbour classification. The cluster centres are updated and the process continues until none of the patterns changes class membership. The clustering procedure is taking into consideration all AE parameters in finding the suitable numbers of classes.

**RESULTS**

**Materials with maximum grain size up to 0.5 mm**

The four materials A5, A50, A200 and A500 were tested with the disk irradiation method and the AE were recorded during the thermal shock (more information about these results can be found in the paper [7]). The purpose of changing the maximum grain size in the four materials was to provoke different fracture patterns. More than ten test pieces were tested of each material in order to check the repeatability of the results. After having been tested, each test piece was analysed by scanning electron microscopy (SEM) and computed tomography (CT) at IKGB, Freiberg, Germany to identify the prevailing fracture patterns.

According to the SEM analyses of the materials A5, A50 and A200, these materials showed a typical failure pattern with one crack which proceeds only through the matrix. The CT analysis also showed, for all test pieces, only one pronounced crack which started at the edge of the test piece and ended roughly in the middle. Accordingly, crack initiation and matrix cracking were identified as the two prevailing failure mechanisms.

SEM analysis of the material A500 established that cracks proceeded through the matrix, but also between the grains and the matrix (decohesion). Accordingly, it was concluded that crack initiation, matrix cracking and decohesion were the three prevailing failure mechanisms.

The AE analyses from materials A5, A50 and A200 showed that, when trying to cluster the AEs into different numbers of clusters, best results were obtained with clustering into two clusters. The AE analysis from material A500 showed that, when trying to cluster the AEs into different numbers of clusters, best results were obtained with clustering into three clusters

**Material with a maximum grain size from 0.5 mm to 6 mm**

The four materials A05-F, A1-F, A3-F und A6-F were tested the same way using the disc irradiation method and the AE were again recorded during the thermal shocks. More than ten test pieces were tested of each material in order to check the repeatability of the results. Each tested test piece was afterwards analysed by scanning electron microscopy (SEM) at IKGB, Freiberg, Germany to identify the prevailing fracture patterns.

The SEM analysis of the material A05-F established that cracks proceeded through the matrix, but also between the grains and the matrix (decohesion) (Figure 4). Accordingly, it was concluded that crack initiation, matrix cracking and decohesion were the three prevailing failure mechanisms.

According to the SEM analyses of the materials A1-F, A3-F and A6-F, these materials showed a failure pattern with only one crack which proceeded through the matrix, between the grains and the matrix (decohesion) but also through the grains (Figure 5). In agreement with these analyses it was concluded that crack initiation, matrix cracking, decohesion and transgranular fracture were the four prevailing failure mechanisms.

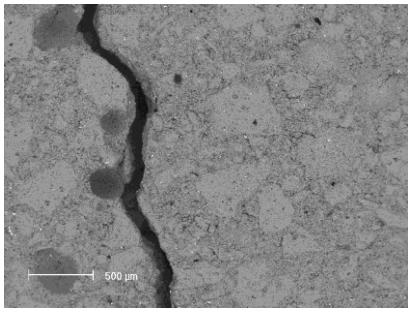


Fig. 4: SEM analysis of the material A05-F after a thermal shock.

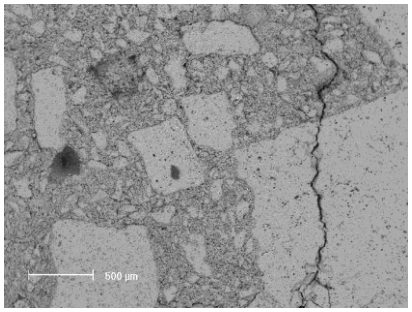


Fig. 5: SEM analysis of the material A3-F after a thermal shock.

Figures 6, 7 and 8 show the classification of the AE signals for the material A05-F. Figures 6 and 7 give the distribution of AE amplitude and the AE energy distribution over time plotted on a logarithmic scale (see Figure 3 for description of AE parameters). Figure 8 shows the distribution of AE duration as a function of AE amplitude plotted on a logarithmic scale. When trying to cluster the AEs into different numbers of clusters, best results were obtained with clustering into three clusters (named "A class", "B class" and "C class"). It should be noted again that the clustering procedure is applied on all different AE parameters of each AE concurrently, not only on the one of the AE parameters as shown in Figures 6 or 7.

The first AE was generally detected approximately 34,45 s after turning on the halogen lamps ("A class"). The temperature gradient in the test pieces at this point was about 218 K. The amplitude of this first AE was always high and in the range of 80 to 90 dBae (for all tested specimen from material A05-F). Furthermore, the AE duration was up to 70000 µs. After a pause of approximately 0.05 s, AEs appeared in quick succession and were divided into two different classes. A number of hits were identified as "C class" with AE amplitude between 37 and 43 dBae, AE duration between 1500 and 2000 µs and AE energy between 7 and 40. They were followed immediately by AEs identified as "B class" with low AE amplitude (< 45 dBae), low AE signal energy (< 10) and low AE duration (< 1500 µs).

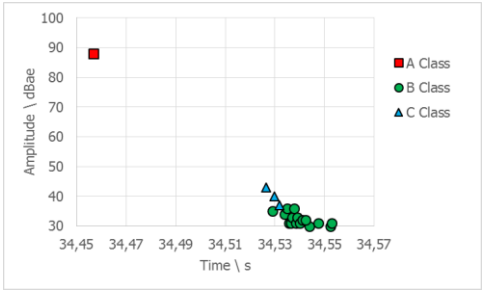


*Fig. 6: Distribution of AE amplitude over time for material A05-F.*

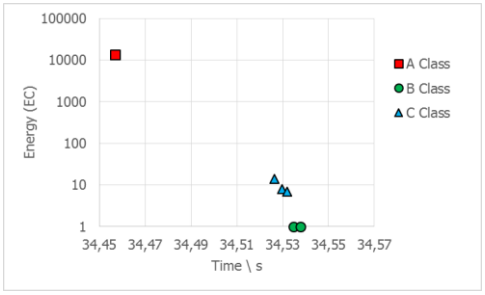


Fig. 7: Distribution of AE energy over time for material A05-F.

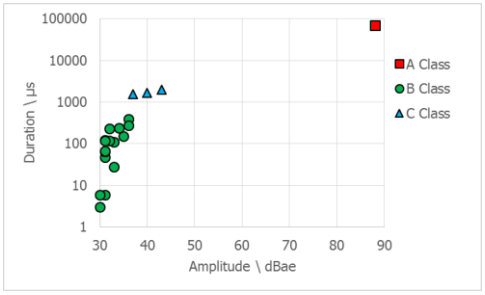


Fig. 8: Distribution of AE duration as a function of AE amplitude for material A05-F.

Figures 9, 10 and 11 show the classification of the AE signals for the material A3-F. These figures give the AE amplitude and the AE energy distribution over time (Figures 9 and 10). Figure 11 shows the distribution of AE duration as a function of AE amplitude. Best results were obtained with clustering the AE into four clusters (named "A class" to "D class").

The first AE were recorded approximately 16,7 s after turning on the halogen lamps ("A class"). The temperature gradient in the test piece at this point was about 155 K. The amplitude of this first AE was always high and in the range of 75 to 85 dBae (for all tested specimen from material A3-F). Furthermore, the AE duration was up 50000 µs. After 0.05 s on average, AEs appeared in quick succession and were divided into three different classes. Few AEs were identified as "D class" with AE amplitude between 45 and 50 dBae, AE duration from 4500 to 20000 µs and AE energy from 30 to 300. A number of hits were identified as "C class" with AE amplitude between 40 and 44 dBae, AE duration between 1200 and 4000 µs and AE energy

between 10 and 25. They were followed immediately by AEs identified as "B class" with low AE amplitude (< 40 dBae), low AE signal energy (< 10) and low AE duration (< 1200 µs).

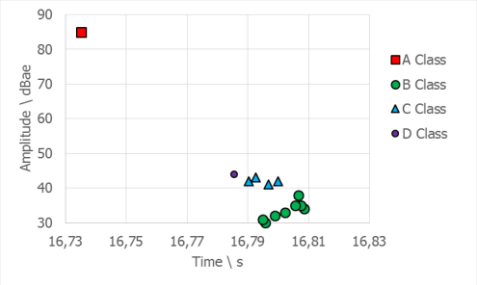


Fig. 9: Distribution of AE amplitude over time for material A3-F.

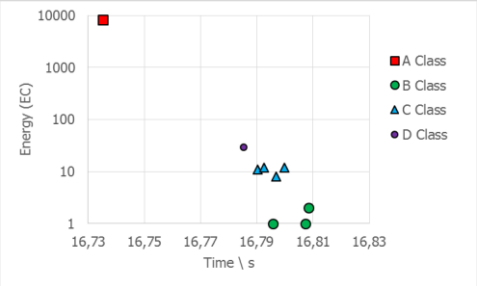


Fig. 10: Distribution of AE energy over time for material A3-F.

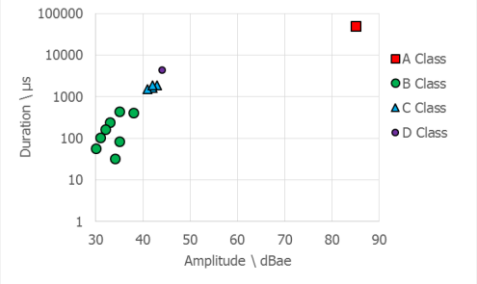


Fig. 11: Distribution of AE duration as a function of AE amplitude for material A05-F.

## CONCLUSIONS

Thermal shock tests were performed on a first series of test pieces made from four different alumina-based materials with different maximum grain sizes up to 500 microns, while concurrently monitoring the acoustic emissions during thermal shock. SEM and CT analysis of the specimens after thermal shock showed that two or three different fatigue/crack mechanisms were involved (matrix cracking, crack initiation and sometimes debonding). The acoustic signals collected during these tests were analysed using a multi-parameter classification method. Results showed that two or three distinct classes of acoustic signatures could be identified.

The second series of thermal shock tests were performed on test pieces made from four different alumina-based materials with maximum grain size between 0.5 and 6 mm. SEM analysis of the specimens after thermal shock showed that three or four different fatigue/crack mechanisms were involved (matrix cracking, crack initiation, debonding and sometimes transgranular cracks). The acoustic signals collected during these tests were again analysed using a multi-parameter classification method and results showed likewise that it was possible to identified three or four distinct classes of acoustic signatures.

By observing the AEs recorded, it was noted that the first AE shows different properties for each material. As a matter of fact, the more the maximal grain size was increased, the faster the crack appeared after turning on the halogen lights and the lower the temperature difference between the center and the side of the test piece at the moment of the AE was. The temperature difference amounted to more than 227 °C for material A05-F and only to 70 °C for material A6-F.

In accordance with these results, the more the maximal grain size was increased, the lower the AE energy released was. The AE released was higher than 19 900 for the material A05-F and only 3 100 for the material A6-F.

The value obtained for the AE amplitude of the first AE was found to be in conformity with the previous results. The AE amplitude was 87,5 dBae for the material A05-F and 75 dBae for the material A6-F.

Additionally it was observed that, with increasing maximum grain size up to 6 mm, the failure mechanism by cracks propagating through the refractory grains (transgranular) during the thermal shock became more important.

In summary it was concluded:

- Increasing the maximum grain influenced the AE.
- Increasing the maximum grain size significantly raised the number of defects. This implies the displacement of the fracture pattern from fractures only propagating through the matrix to propagation through the grains and at the interface between the grains and the matrix (delamination).
- The more the maximal grain size was increased, the earlier the first AE showing cracking appeared and the lower the temperature difference between the centre and the side of the test piece at this moment was. This was explained again by the increase of the number of defects, when the maximal grain size was increased. Therefore, the material was expected to show lower resistance to crack initiation.


## ACKNOWLEDGEMENT

We would like to thank the German Federation of Industrial Research Associations (AiF) for its financial support of the research project IGF No. 18732 BG. This project was carried out under the auspices of AiF and financed within the budget of the Federal Ministry of Economic Affairs and Energy (BMWi) through the programme to promote collective industrial research (IGF).


## REFERENCES


[1] Kostopoulos V, Loutas T, Dassios K. Fracture behaviour and damage mechanis identification of SiC/glass ceramic composites using AE monitoring. Composites Science and Technology. 2007. 67: 1740-1746.

[2] Masmoudi S, El Mahi A, Turki S, El Guerjouma R. Structural Health Monitoring of Smart Composite Material by Acoustic Emission. Société Francaise d'acoustic. Acoustics 2012, Nantes. 71-76.

[3] Loutas TH, Kostopoulos V. Healt monitoring of carbon/carbon, woven reinforced composites. Damage assessment by using advanced signal processing techniques. Part I: Acoustic emission monitoring and damage mechanisms evolution. Composites Science and Technology. 2009. 69: 265-272.

[4] Kempf M, Skrabala O, Altstädt V. Acoustic emission analysis for characterization of damage mechanisms in fibre reinforced thermosetting polyurethane and epoxy. Composites. 2014. B 56: 477-483.

[5] Schneider GA. Thermoschockverhalten von Hochleistungskeramik. Dissertation, Universität Stuttgart. 1989.

[6] Brochen E, Clasen S, Dahlem E, Dannert C. Determination of the thermal shock resistance of refractories. refractories WORLDFORUM. 2016. 8: 79-85.

[7] Dahlem E, Dannert C, Werner J, Aneziris C. Failure process of refractory materials during thermal shock evaluated by acoustic emissions. 59th International colloquium on refractories, September 28th and 29th, 2016, Aachen, Germany.